Cell. Mol. Biol. (ISSN: 1165-158X)

Journal Homepage: www.cellmolbiol.org

Cellular and Molecular Biology

Original Article

Development and characterization of polysiloxane-based gel loaded with phyto-ingredients encapsulated in phytosomes for scar management

Tahereh Naseriyeh[1], Danial Kahrizi[1*], Elham Arkan[2], Sajad Moradi[2], Farzad Kahrizi[3]

[1] *Nanobiotechnology Department, Faculty of Innovative Science and Technology, Razi University Kermanshah, Iran*
[2] *Nano Drug Delivery Research Center, Health Technology Institute, Kermanshah University of Medical Sciences, Kermanshah, Iran*
[3] *Department of Pharmacology and Toxicology, Faculty of Pharmacy, Damghan Branch, Islamic Azad University, Damghan, Iran*

Article Info

Article history:

Received: September 26, 2023
Accepted: August 14, 2024
Published: August 31, 2024

Use your device to scan and read the article online

Abstract

Recent research has emphasized the development of efficient drug delivery systems to facilitate the delivery of biological compounds such as polyphenols via skin absorption. Phytozomes have been employed as carriers of plant compounds in this context Hydrogen bonding between plant polyphenols and the phospholipid phosphate group enables efficient encapsulation of potent compounds for enhanced drug delivery systems. Additionally, the strong affinity of phytosomes for the skin's phospholipids enhances skin absorption. In this study, phytosomes were initially formulated using the thin-layer hydration method After optimizing the synthetic parameters, phytosomes were loaded with Resveratrol and Quercetin for enhanced delivery and skin absorption potential to assess the characteristics of the synthesized phytosomes, tests were conducted to determine particle distribution and size, zeta potential, and examine the microstructure morphology using a scanning electron microscope (SEM). Furthermore, a siloxane gel base was formulated in this study, and the stability of the physicochemical and biological properties of the final prepared nanoformulation was investigated. The results of this study indicated that the formulated phytosomes exhibit optimal characteristics for facilitating high skin penetration of resveratrol and quercetin. A high skin absorption was observed after 60 days of synthesis. Additionally, the base of the siloxane gel can play a significant role in preventing the formation of scars by reducing the passage of water vapor.

Keywords: Scar, Phytosomes, Resveratrol, Quercetin, Dermal absorption

1. Introduction

Scar formation is the result of the inevitable process of wound healing and an imbalance between fibrogenesis and fibrolysis. After skin damage, the reconstruction of dermis and epidermis structures takes place during the wound healing process in the stages of homeostasis, inflammation, proliferation, and regeneration [1,2]. At the onset of skin damage, with immediate hemostasis, degranulated platelets initiate the coagulation cascade to form a fibronectin-fibrin clot. This clot acts as a scaffold, not only preventing wound bleeding but also facilitating the wound-healing process by creating a chemotactic gradient [3]. Following the establishment of homeostasis, signals produced by DAMPs, PAMPs, chemokines (such as CXCL7, CXCL4, CXCL1, CXCL5, CCL5, CCL3), and cytokines (such as platelet-derived growth factor (PDGF) and transforming growth factor β (TGFβ) trigger the migration and activation of inflammatory cells such as macrophages and neutrophils in the injury area. These cells serve a dual purpose by not only safeguarding against infection but also aiding in the clearance of necrotic tissue. Moreover, the activated cells involved in the inflammatory response release chemokines and cytokines that are pivotal in advancing the proliferation phase. The proliferation of fibroblasts increases due to the influence of PDGF and TGF β 1 secreted from macrophages, leading to an increase in the production and deposition of collagen type III by these cells [4]. Macrophages, through the secretion of platelet-derived growth factor (PDGF) and transforming growth factor beta 1 (TGFβ1), induce fibroblasts to proliferate and produce and deposit type III collagen [5]. In the proliferation phase of wound healing, granulation tissue develops, comprising macrophages, fibroblasts, and endothelial cells, replacing the initial hemostatic plug. Under the influence of transforming growth factor β1 (TGFβ1), certain fibroblasts differentiate into myofibroblasts, exhibiting distinctive contractile capabilities. Myofibroblasts, which are typically temporally and spatially restricted in the normal wound healing process, exhibit sustained presence in fibroproliferative scars and hypertrophic scars [6]. The progression towards scar formation and maturation primarily occurs due to an increase in the total number of crosslinks between

* Corresponding author.
E-mail address: ddkahrizi@modares.ac.ir (D. Kahrizi).
Doi: http://dx.doi.org/10.14715/cmb/2024.70.8.32

extracellular matrix (ECM) collagen fibers. This process is pivotal in the remodeling phase of wound healing, leading to the characteristic tissue restructuring associated with scar formation. During the regeneration phase of wound healing, type I collagen gradually displaces type III collagen, leading to the replacement of damaged tissue with a type I collagen-rich matrix. This transition culminates in the formation of organized collagen tissue characteristic of scar formation Moreover, the compromised epidermis, experiencing abnormal water loss post-injury, prompts epidermal keratinocytes to release inflammatory cytokines, subsequently enhancing collagen synthesis by fibroblasts [7]. Various factors contribute to scar formation during the wound healing process, such as the extent and severity of the inflammatory response, aberrant fibroblast-myofibroblast transition, inadequate apoptosis of fibroblasts, and excessive collagen accumulation [8, 9]. Indeed, modern scar management and treatment options encompass a range of strategies aimed at improving scar appearance and functionality [10], 5-Flurouracil injection into the scar [11], laser [12], cryotherapy [13], radiotherapy [14] and surgery [15], which are often associated with side effects that cannot be overlooked. Silicone-based treatments are favored for scar management due to their relatively lower incidence of serious side effects compared to other modalities. Additionally, they are often considered more effective in scar reduction and improving scar appearance [16, 17]. Silicone-based products function by maintaining hydration in the wound, thereby preventing epidermal dehydration and keratinocyte activation. This mechanism inhibits the excessive collagen deposition that contributes to scar formation [18, 19]. Combining silicone-based treatments with therapeutic phytochemicals presents a promising therapeutic strategy due to the anti-inflammatory and anti-scarring properties of phytochemicals. This synergistic approach may enhance scar management outcomes by addressing both inflammation and collagen deposition in the wound-healing process. Resveratrol (Res) and Quercetin (Que), well-known polyphenols, have garnered attention for their anti-scar properties. Research focusing on human scar hypertrophic fibroblasts (HSFBs) indicates that Res treatment induces cell cycle arrest, promotes apoptosis, and inhibits cell proliferation. Additionally, Res prevents the formation of collagen deposits by reducing the expression of type I and III collagen in HSFBs [20]. One of the signaling pathways that play a key role in scar formation is the TGF-β1/Smad pathway. Res prevents scar formation by reducing the expression of TGF-β1 and Smad-2, 3, and 4 proteins [21]. Res has been shown to downregulate key components of the mTOR signaling pathway, including PI3K and AKT, which are typically upregulated in human scar HSFBs. This modulation may contribute to the anti-scar properties of Resveratrol by influencing cellular processes involved in scar formation [22]. The impact of Res on modulating key molecular signaling pathways, such as TGF-β1/Smad and mTOR, presents a novel and promising therapeutic strategy for addressing pathological scar formation. By targeting these pathways, Res shows potential in mitigating scar formation through its multifaceted mechanisms of action. Que has demonstrated efficacy in preventing scar formation at the cellular level. Studies have shown that Que reduces fibroblast proliferation in keloid scars and diminishes collagen synthesis through modulation of intracellular signaling pathways. Que exerts its anti-scarring effects by inducing cell cycle arrest and apoptosis in fibroblasts. Additionally, it also contributes to preventing scar formation by improving collagen organization, a crucial factor in scar appearance and tissue remodeling This effect on collagen structure may play a significant role in reducing scar formation and promoting better wound healing outcomes [23]. While these phytochemicals offer significant therapeutic benefits, their stability can be compromised by exposure to environmental factors like temperature, humidity, light, and oxygen levels. This susceptibility to environmental changes may impact the efficacy of the phytochemicals [24]. Phytosomes, a phospholipid-based delivery system resembling liposomes, offer a solution to the stability challenges of phytochemicals. They provide a promising method for effectively delivering plant polyphenolic compounds. The formation of a lipid bilayer in phytosomes can enhance the absorption of hydrophobic compounds, enabling improved bioavailability and efficacy of the delivered phytochemicals. Phytosomes are constructed with phospholipids, predominantly phosphatidylcholine, through the formation of hydrogen bonds between the polyphenols' phenolic groups and the phospholipids' phosphate group. This unique structure enhances the delivery and absorption of plant polyphenolic compounds, offering potential benefits in therapeutic applications [25]. The exceptional skin penetration capability of phytosomes underscores their significance in enhancing the absorption of polyphenols into the skin. By fostering improved skin uptake of polyphenols, phytosomes offer a promising approach for sustaining the presence of these compounds in the skin over time, potentially benefiting the management of skin disorders and diseases [26].

The integration of phytosomes loaded with Res and Que into a silicone gel base presents a novel combined therapeutic strategy. This approach aims to leverage the benefits of both Res and Que to enhance scar resolution effectively. The synergistic action of these phytochemicals delivered via phytosomes in a silicone gel base holds promise for achieving optimal scar management outcomes.

2. Material and methods

2.1. Materials

Resveratrol, quercetin, siloxane, phosphatidylcholine and MTT were purchased from Sigma-Aldrich, Germany. Ethanol and chloroform were purchased from Merck, Germany. T25 filter flask, T75 filter flask, Dialysis membrane, PBS, 24 and 96-Well Plates were purchased from Chemia Rahavard, Iran, and Trypsin and DMEM medium were purchased from Bioidea, Iran. MCF-7-7 cell line and Fibroblast cell line Pasteur Institute, Iran.

2.2. Synthesis Res-Que-Phytosomes

To prepare phytosomes containing Res and Que, first, 20 mg of phosphatidylcholine was dissolved in 500 microliters of chloroform. Then, 9 mg of Res was dissolved in 300 microliters of ethanol and 3 mg of Que in 200 microliters of ethanol were added to the phosphatidylcholine solution. A homogeneous solution was obtained, which was kept at 4°C for 24 hours. After 24 hours, the resulting solution was placed in a rotary evaporation device with a temperature of 50 degrees Celsius and a rotation speed of 150 rpm for 30 minutes to evaporate the solvent. After complete evaporation of the solvent, a thin film layer of lipid was formed on the wall of the glass balloon. Then, 20

ml of distilled water at a temperature of 50°C was added to the balloon containing the thin lipid film and placed in a sonication bath for 5 minutes. The milky-colored suspension involves phytosomes containing Res and Que. The resulting phytosomes suspension was placed in an ultrasound bath for 5 minutes and then the sonicator probe was used 3 times at 70 kHz for 3 minutes with a time interval of 5 minutes. Subsequently, it was placed in the ultrasound bath for an additional 3 minutes. Finally, the resulting suspension was centrifuged at 8000 rpm for 10 minutes at 4°C to collect the phytosomes, which were then stored at 4°C.

2.3. Characterization of Res-Que-Phytosomes

2.3.1. Measurement of hydrodynamic diameter and zeta potential of Res-Que phytosomes

(Malvern Instruments Ltd., USA) was employed to determine the hydrodynamic diameter (DLS) and zeta potential of Res-Que phytosomes.

2.3.2. Investigating the morphology and size of Res-Que phytosomes

Scanning electron microscope (SEM) images were utilized to determine the precise size of Res-Que phytosomes. Beyond size measurements, SEM images were instrumental in evaluating the morphology of the Res-Que phytosomes.

2.3.3. Measurement of resveratrol and quercetin loaded in Res-Que phytosomes

Drug loading (DL) and encapsulation efficiency (EE) of Res and Que in the phytosomes were assessed by quantifying the levels of free Res and free Que in the supernatant obtained post-centrifugation, utilizing UV-vis spectrophotometry at 310 nm for Res and 370 nm for Que. DL and EE were calculated using specific Equations (1 and 2) based on the measured concentrations of the free drugs and the initial drug amounts added during phytosome preparation.

Drug Loading

$$= \frac{\text{mass of Res or Que in phytosomes}}{\text{mass of Res-Que phytosomes}} \times 100 \qquad \text{Equations 1}$$

Entrapment Efficiency

$$= \frac{\text{mass of Res or Que in nanoparyicle}}{\text{mass of total Res or Que}} \times 100 \qquad \text{Equations 2}$$

2.3.4. Fourier-transform infrared spectroscopy (FTIR) study

For FTIR spectral analysis, powders of lecithin, Res, quercetin and Res-Que phytosomes were mixed with KBr and prepared as tablets. Subsequently, the spectra were acquired in the range of 400-4000 cm^{-1}. to examine the chemical characteristics and interactions present in the samples.

2.3.5. Measurement of Res and Que release from Res-Que phytosomes in vitro

The in vitro release of Res and Que from Res-Que phytosomes was investigated in a physiological pH of 7.2 buffer environment. 250 micrograms of Res-Que phytosomes containing 63 micrograms of Res and 24 micrograms of Que (the loading rate was 25.4% and 9.6%, respectively) were added to 1ml of buffer and placed in a dialysis bag with a cut-off of 12 kilodaltons. The dialysis bag was then immersed in the designated environment. The release rate of Res and Que was monitored for 12 hours, with 1 ml of the buffer medium being replaced every hour with fresh buffer. After sampling, the absorption of the samples was measured at wavelengths of 310 nm for Res and 37 nm for Que, and the values were reported as percentages. The experimental study was carried out with a repetition of n=3, indicating that each experimental condition and measurement was replicated three times to ensure the reliability and robustness of the results obtained for the release behavior of Res and Que from the Res-Que phytosomes.

2.4. Selecting the appropriate polymer for creating the siloxane gel base

Siloxane, which is in liquid form, is typically combined with a compatible polymer to create a gel base. In this investigation, various synthetic polymers such as polyacrylonitrile (PVA) and carboxymethyl cellulose (CMC), as well as natural polymers like tragacanth and starch, along with emulsifiers Tween and Span, were explored for formulating the siloxane gel. The percentage of polymers used was as follows: PVA (2%, 4%, and 8%), CMC (75%, 1.5%, and 3%), tragacanth (25%, 5/0, and 1%) and starch (2%, 4%, and 8%). Following the selection of polymers, they were blended with siloxane polymer in three proportions: A (equal ratio of siloxane to polymer), B (25% ratio of polymer to siloxane), and C (75% ratio of polymer to siloxane). Monitoring was conducted weekly over a 4-week duration to assess turbidity and phase separation characteristics, aiming to establish a visually clear and uniform gel base suitable for the intended application.

2.5. Synthesis of siloxane gel base containing Res-Que phytosomes

A specific ratio of siloxane, tragacanth (25%), and Tween 80 (1:1:0.25, respectively) was employed to establish the base of the siloxane gel. Then equal proportions of tragacanth siloxane along with 10% v/v of tween were thoroughly mixed with a stirrer for better stabilization. In order to obtain a 10% w/v volume ratio of effective compounds in the final gel, 300 mg of phytosome containing resveratrol and quercetin was added per milliliter of the final gel.

2.6. Measuring the amount of water vapor passage

In order to quantify the water vapor permeability a layer of parafilm was glued on the opening of a cylindrical glass containing water and completely identical holes were created on the parafilm. Following this, the gels and compounds were positioned on top of the mesh parafilm. The study involved 5 defined groups: a control group, Dermalift product group, Scar Gel product group, tragacanth, and tragacanth-siloxane. The cylindrical glass from each group was then placed in an incubator set at a constant temperature of 37˚Cand a relative humidity of 50%.

2.7. Cell cytotoxicity assay

Fibroblasts were seeded (2000 cells per well) in 96-well plates and incubated in DMEM medium (containing 10% FBS, 0.25 µg/ml amphotericin, 100 µg/ml streptomycin, and 100 U/ml penicillin). The in vitro cytotoxicity study involved the definition of four distinct groups. The

defined groups involve control (without treatment), free Res (65 µg/ml) and free Que (25 µg/ml), Res-Que phytosomes, and Res-Que phytosomes-Gel. After 24 hours of treating the groups, the MTT test was used to determine the effect of these compounds on cell survival. At the end of the incubation time, MTT solution with a concentration of 5 mg was dissolved in one ml of PBS buffer and added to each well. 25 µL were added in a ratio of 1 to 10. Then the plates were placed in the incubator for 4 hours, during which the succinate dehydrogenase enzyme present in the mitochondria of living cells regenerated the bromine element in the MTT solution and converted it into purple formazan crystals. Since these particles are insoluble, 100 µL of pure dimethyl sulfoxide solution was added to each well to dissolve the formazan crystals. The plate was then incubated in the dark for 15 to 20 minutes. Finally, the absorbance of the samples was read and recorded at a wavelength of 570 nm.

2.8. Dermal absorption assay

Rat skin was used in this study. The rats used in this research project were of the Sprague–Dawley breed and weighed 100–150 g. All animals were kept under identical conditions before the experiment. The storage conditions included polycarbonate cages containing the same food and water. First, the animal was anesthetized with chloroform in a desiccator and then sacrificed (by cutting its spinal cord). The entire abdominal region of the animal, spanning from below the chest to the top of the pelvis, was entirely devoid of hair. The skin of this area was then completely separated, and the fat under the skin was removed and kept in normal saline solution until use. To maintain the skin's physicochemical and biological properties and simulate in vivo conditions, freshly prepared skin was utilized for each experiment. The time interval between skin removal from the animal's body and placement in the diffusion cell did not exceed 1 hour. The French diffusion cell was loaded with 30 ml of buffer (stirred at 70 rpm, maintained at a temperature of 37 ± 2.5 °C), and the skin, with a natural membrane area of 1 x 1 cm^2, was positioned on top of the buffer solution. In the skin absorption study, two groups were established. In one group, the skin was treated with 1 mg of Res-Que phytosomes-gel, equivalent to 250 micrograms of phytosomes. Based on the loading percentage of Res and Que, there are 63.5 µg of Res and 24 µg of Que in 250 µg of Res-Que phytosomes. In the other group, 250 µg/ml (physiological buffer) of Res-Que phytosomes was applied to the skin. For both groups, 1 ml of sample was withdrawn from the Franz cell every hour for 12 hours and replaced with 1 ml of buffer. The levels of Res and Que in the samples were assessed using UV spectroscopy at wavelengths of 310 nm for resveratrol and 370 nm for quercetin. To evaluate the stability of Res-Que phytosomes-gel after 60 days, the skin absorption of Res and Que was examined using the same measurement protocol as on the initial day.

2.9. Data statistical analyses

The data collected was analyzed using Excel version 2020 and Prism GraphPad. Results from each group were expressed as mean ± standard deviation (Mean ± SD). Group comparisons were performed utilizing one-way analysis of variance (ANOVA) and t-tests. Graphical representations were generated using Prism GraphPad software, with statistical significance defined at $p < 0.05$.

3. Result

3.1. Characterization of Res-Que phytosomes

Based on the results, the hydrodynamic diameter of the empty phytosomes measures 80 nm (Figure 1A). Upon the incorporation of Res and Que into the phytosomes, forming Res-Que phytosomes, the hydrodynamic diameter expanded to 110 nm (Figure 1B), demonstrating the effective loading of resveratrol and quercetin into the phytosomes. The zeta potential of the empty phytosomes was measured at -35 mV (Figure 2A). Following the addition of Res and Que to the phytosomes, the zeta potential decreased to -29 mV (Figure 2B). The size of Res-Que phytosomes was assessed using SEM imaging. Figure 3 displays the spherical morphology of the Res-Que phytosomes, providing insights into their size characteristics.

In the spectral analysis of Res, the peaks at 13230 cm^{-1}, 11604 cm^{-1}, 11589 cm^{-1}, 11513 cm^{-1}, and 1461 cm^{-1} correspond to stretching of O-H, C=C, C-C (olefinic), benzene ring vibration, and in-plane bent O-H, respectively. In the spectrum collected from Que, the O-H stretch was observed at 13400 cm^{-1}, the C-H stretch at 12930 cm^{-1}, the C=O

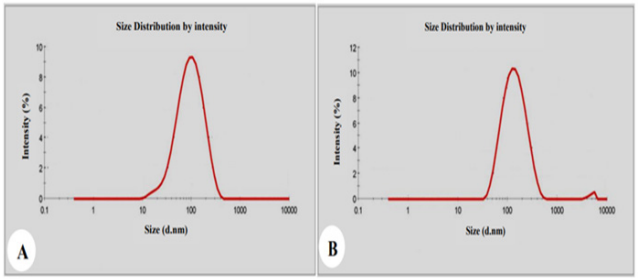

Fig. 1. Hydrodynamic diameter of empty nano-phytosome (A) and hydrodynamic diameter of nano-phytosome containing Res and Que (B).

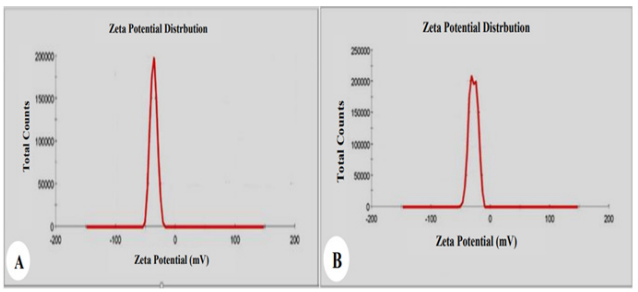

Fig. 2. Zeta potential of empty nano-phytosome (A) Zeta potential of nano-phytosome containing Res and Que (B).

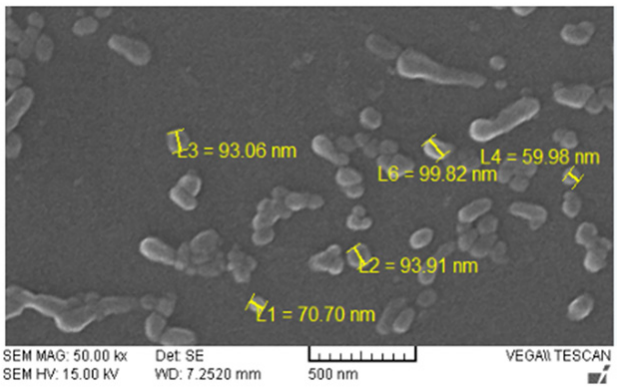

Fig. 3. SEM imaging of nano-phytosome containing Res and Que.

stretch at 11680 cm^{-1}, the aromatic C=C stretch at 11510 cm^{-1} and 1610 cm^{-1}, and the aromatic C-O stretch at 1220 cm^{-1}. The CH3 and CH2 stretch bond vibration peaks were shifted from their original positions in lecithin (12850 cm^{-1} and 2956 cm^{-1}) to higher wave numbers in Res-Que phytosomes (12853 cm^{-1} and 2970 cm^{-1}) Figure 4.

The drug loading (DL) and effective encapsulation (EE) values for Res are 25.4% and 70%, respectively, while for Que they are 9.6% and 80%, respectively. The release rates of Res and Que from Res-Que phytosomes were studied over 12 hours, with each measurement repeated three times. The release rate of Res from Res-Que phytosomes was 78% (Figure 5A), while the release rate of Que from Res-Que phytosomes was 82% (Figure 5B).

3.2. Selecting the appropriate polymer for creating the siloxane gel base

Based on the results, among the selected percentages, PVA (4%), CMC (1.5%), tragacanth (25%), and starch (4%) exhibited the optimal viscosity for a gel base formulation.

In the study, six groups of polymers were tested to determine the optimal gel base percentage. The emulsifier amount (Tween80 and Span) was maintained at 10% v/v siloxane and tragacanth. The ratios tested were: 1 (equal polymer to siloxane with Tween80), 2 (25% polymer to siloxane with Tween80), 3 (75% polymer to siloxane with Tween), 4 (equal siloxane to polymer with Span), 5 (25% polymer to siloxane with Span), and 6 (75% polymer to siloxane with Span). The gel bases were monitored for characteristics such as stability, turbidity, and phase separation over four weeks.

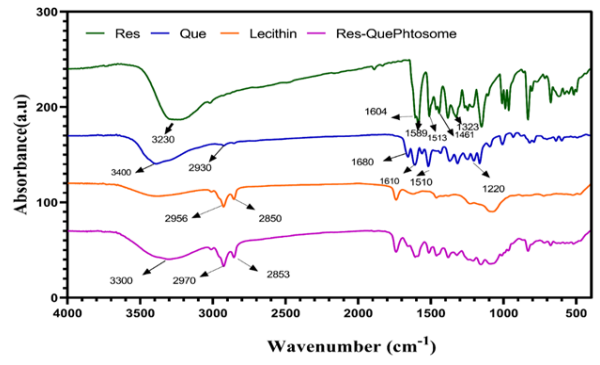

Fig. 4. The peaks obtained from Res, Que, lecithin, and phytosomes containing Res and Que.

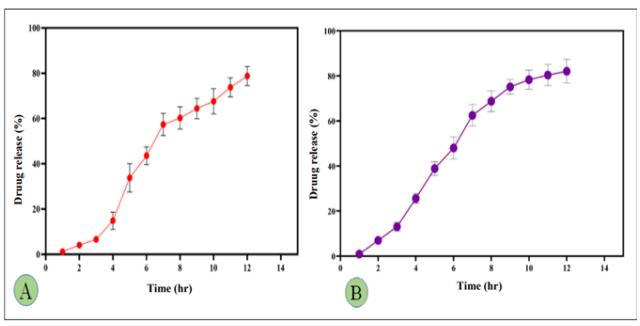

Fig. 5. Release rate Res (A) release rate Que (B).

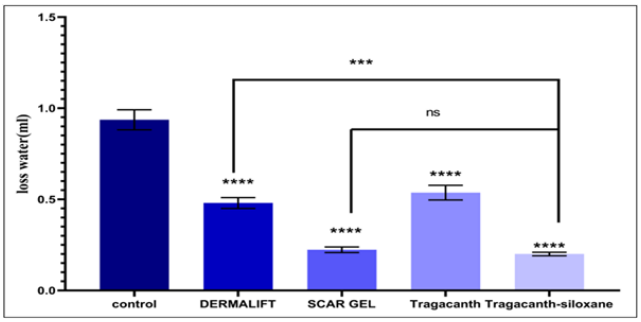

Fig. 6. Investigating the performance of tragacanth-siloxane gel base in preventing the passage of water vapor with 4 groups: a control, Dermalift product group, Scar Gel product group and tragacanth.

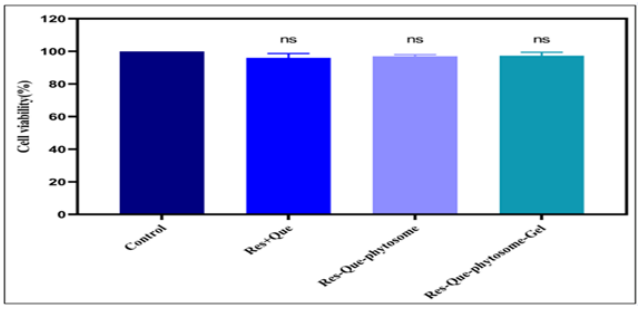

Fig. 7. Investigation of cytotoxicity on the fibroblastic cell line.

3.3. Investigating the performance of tragacanth-siloxane gel base in preventing the passage of water vapor

Since one of our goals is to create a gel base that prevents water evaporation, we investigated the amount of water evaporation from the gel produced. As depicted in Figure 6, statistically, the amount of water vapor passing through the tragacanth-siloxane gel base is significantly reduced compared to the Dermalift product ($P < 0.0001$). However, the basic performance of the tragacanth-siloxane gel is not significantly different from that of Scar Gel; in fact, the two products have the same effect Figure 6.

3.4. The effect of Res-Que phytosomes-Gel on fibroblasts viability

The investigation into the cytotoxic effect of Res-Que phytosomes-gel on fibroblast cells, as illustrated in Figure 7, indicated no significant difference between the control group and the groups treated with Res and Que. Additionally, there was no notable variance between the control group and the groups exposed to Res-Que phytosomes and Res-Que phytosomes-Gel.

3.5. The effect of Res-Que phytosomes-Gel on dermal absorption of Res and Que

After conducting a statistical analysis of the results obtained from measuring the skin absorption of Res and Que, it was observed that the tragacanth-siloxane gel base does not interfere with the skin absorption of these compounds (Figures 8 and 9). As illustrated in Figure 8, the absorption of Res increases in the first 2 to 3 hours, peaks at 6 hours, and then stabilizes thereafter.

The amount of Que absorption has increased significantly in the first 2 hours and reaches its peak at 4 hours. After 4 hours, the absorption amount remains constant Figure 9.

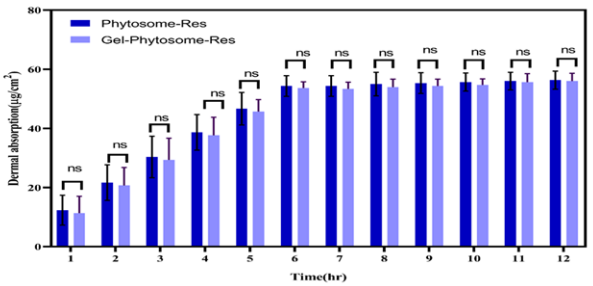

Fig. 8. Skin absorption graph of Res in 12 hours.

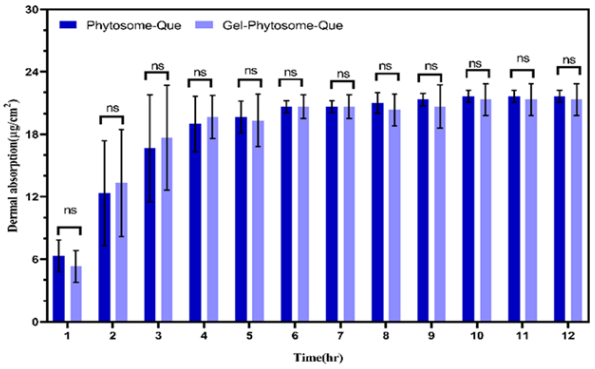

Fig. 9. Que skin absorption graph in 12 hours.

To assess the stability of Res-Que phytosomes-gel after 60 days of synthesis, the release of Res and Que was measured. (Figure 10 and Figure11) illustrate that after 60 days, there was no significant alteration in the release of these compounds. Therefore, it can be inferred that Res-Que phytosomes-gel exhibits good stability.

4. Discussion

In this study, Res-Que phytosomes-gel was synthesized and characterized in vitro. Additionally, the synergistic effects of polyphenols and silicone-based gel in the treatment and management of scars were investigated in vitro. To enhance the stability of resveratrol and quercetin, they were loaded into phytosomes. Similar to other therapeutic nanoparticles, factors such as size and surface charge play a crucial role in the stability and efficacy of phytosomes. The decline in zeta potential of Res-Que phytosomes to unloaded phytosomes indicates potential electrostatic interactions between the positively charged phenolic compounds and the negatively charged phosphate groups found in phosphatidylcholine and lecithin. These factors also play a crucial role in determining the strength and mechanism of skin absorption of nanoparticles. A high zeta potential enhances electrostatic repulsion force, and stability, and prevents particle accumulation over time. As the total charge on the particles increases, they repel each other, thereby preventing agglomeration. Therefore, measuring zeta potential is crucial for controlling the agglomeration and deposition of phytosomes. Zeta potential, which is associated with the surface charges of nanoparticles, significantly influences the interaction of nanomaterials with skin components. According to various studies, it has been found that negatively charged vesicles promote higher flux than their positively charged counterparts and enhance drug localization in the skin's surface layers [27-29] . In the collected spectra from the FT-IR study, the loading of Res and Que in phytosomes was demonstrated. The CH3 and CH2 stretch bond vibration peaks were shifted from their original positions in lecithin (12850 cm-1 and 2956 cm^{-1}) to higher wave numbers in Res-Que phytosomes (12853 cm^{-1} and 2970 cm^{-1}). The observed spectral shifts suggest the integration of these polyphenols into the hydrocarbon chains of the lecithin molecule, resulting in the reorganization of CH2 groups and alterations in the associated C-H stretching vibrations. In phytosomes, these polyphenols are likely associated with lipid headgroups either in the core or on the outer surface. The appearance of a peak around 3300 cm-1 suggests that phenolic groups in polyphenol molecules interact with lecithin through hydrogen bonds during the formation of phytosomes structures [30]. In addition to the anti-scarring properties of Que, it plays a key role as a stabilizer of Res. By using a ratio of 3 to 1 for Res and Que, Que Tin plays the stabilizing role effectively. In this study, the amount of Res loading is almost three times that of Que [27]. Next, the optimal ratio of polysiloxane, tragacanth and Tween 80 was chosen to create the siloxane gel base. Silicone-based treatments excel in blocking water vapor passage, a crucial factor in scar prevention. Maintaining hydration in wounds is key to preventing scar formation. In dehydrated conditions, TGFβ stimulates fibroblasts to produce fibronectin and collagen, while FGF increases collagenase levels to regulate collagen synthesis. Siloxane-based products maintain wound hydration, modulate FGF and TGFβ factors, and establish a balance between fibrogenesis and fibrolysis, ultimately preventing scar formation [31]. Edward Dyson and team conducted a study showcasing the superiority of silicone coatings over traditional colloidal coatings. In their in vivo research, patients wearing silicone dressings exhibited significantly lower Trans epidermal Water Loss (TEWL) compared to those wearing hydrocolloid dressings. The TEWL levels approached those of normal skin,

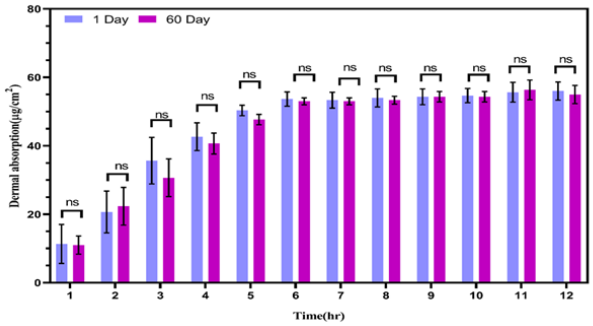

Fig. 10. Investigating the stability of the gel containing phytosome after 60 days of Res skin absorption measurement.

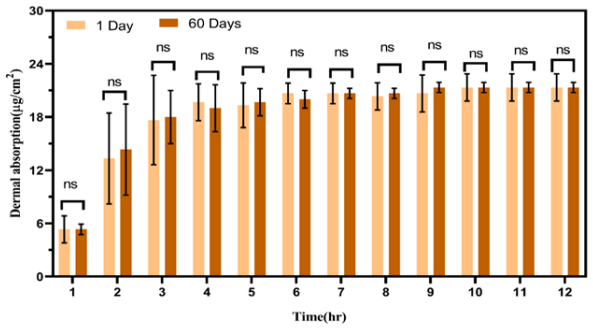

Fig. 11. Investigating the stability of the gel containing phytosome after 60 days of measuring the skin absorption of Que.

indicating a high level of skin occlusion [32]. After investigating the physicochemical characteristics of Res-Que phytosomes-gel, the first step is to assess cellular toxicity in vitro. The lack of cytotoxicity of these compounds can be attributed to the fact that the skin fibroblast cells were exposed to concentrations much lower than the IC50 values reported in other studies for Res and Que [33,34]. The results from the study on dermal absorption confirm the excellent performance of Res-Que Phytosomes Gel. In the analysis of skin absorption, the significance of phospholipids, such as phosphatidylcholine found in lecithin, cannot be overlooked. Phospholipids are essential components of phytosomes, liposomes, and lipid nanoparticles, playing a vital role in their structure and function. The negative charge of phospholipids and the flexibility of their hydrophobic tails play a crucial role in influencing the physical properties of nanoparticles and improving their skin permeability [35,36]. The utilization of lipid nanoparticles containing phosphatidylcholine, particularly lecithin, leads to a notable enhancement in skin absorption compared to therapeutical agents absorption without nanoparticles. This improvement underscores the importance of lipid-based delivery systems in enhancing skin permeability and absorption [37,38]. In the study by Abdi et al., chitosan nanoparticles loaded with bevacizumab were encapsulated with a phospholipid membrane composed of lecithin. As a result of coating chitosan nanoparticles loaded with bevacizumab with a lecithin phospholipid membrane, the skin absorption rate of bevacizumab, despite being hydrophilic, increased to 78% [39]. Lecithin plays a significant role in prolonging the shelf life of compounds in the skin. Certain compounds, despite exhibiting high skin penetration, may have a short shelf life in the skin, which can be addressed by the use of lecithin as a stabilizing agent. For example, the average cumulative penetration of VD3 solution (vitamin D3) was approximately 5.2 times greater than that of VD3 liposomes. Interestingly, the mean retention of VD3 liposomes was 1.65 times higher than that of VD3 solution, indicating the potential role of liposomes, specifically lecithin, in enhancing compound retention in the skin. The swift penetration of VD3 solution into skin tissue highlights its easy permeation; however, its short retention time in the skin underscores the importance of strategies to enhance compound stability and longevity, such as utilizing delivery systems like liposomes with appropriate stabilizing agents like lecithin [40]. In a study conducted by Lorena Maione-Silva et al., negatively charged liposomes increased the skin absorption rate of ascorbic acid from 0.31 µg/cm2/h to 2.19 µg/cm2/h. Additionally, the duration of liposomal ascorbic acid in the skin increased by 5.5 times after 6 hours compared to free ascorbic acid. Additionally, the skin retention time of liposomal ascorbic acid in the skin was extended by 5.5 times after 6 hours in comparison to free ascorbic acid, emphasizing the sustained release and enhanced retention properties of liposomal formulations in skin applications [41]. Phytosomes, akin to liposomes, are instrumental in facilitating the skin absorption of plant polyphenol compounds, attributed to lecithin as a primary component in their structure. For instance, the sinigrin-phytosomes complex at 0.5155 µg/ml significantly increased the skin absorption of sinigrin by sevenfold compared to free sinigrin at 0.0730 µg/ml, highlighting the efficacy of phytosomes in enhancing skin permeation of bioactive compounds [42]. The skin absorption of Res encapsulated in phytosomes exhibited a substantial increase to 54.66% compared to 16.47% for free resveratrol. These findings align with previous research, emphasizing the significant enhancement in skin absorption facilitated by phytosomal delivery systems [43].

5. Conclusion

The results of this study indicate that the physicochemical characteristics of phytosomes incorporating resveratrol and quercetin are favorable, suggesting an optimal formulation for skin absorption and potential therapeutic efficacy. The synthesized phytosomes have the ability to load a high amount of resveratrol and quercetin and also show a high release in the first hours. Incorporating phytosomes into a siloxane gel base offers a promising approach for scar treatment or prevention, potentially enhancing the bioavailability and therapeutic efficacy of bioactive compounds for skin health. Siloxane enhances the efficacy of phytosomes in scar treatment by aiding in the prevention of dehydration of the injured epidermis, thereby promoting skin hydration and improving the overall healing process. In this study, the increase in skin absorption of Res and Que cannot be ignored. The notable enhancement in skin absorption of resveratrol (Res) and quercetin (Que) underscores the potential benefits of incorporating phytosomes loaded with these compounds into a siloxane gel base for scar treatment, highlighting a promising therapeutic approach for skin healing and rejuvenation.

Acknowledgement
We are grateful to Razi University for the financial support of part of this research.

Conflict of Interests
The author has no conflicts with any step of the article preparation.

Consent for publications
The author read and approved the final manuscript for publication.

Ethics approval and consent to participate
No human or animals were used in the present research.

Informed Consent
The authors declare that no patients were used in this study.

Availability of data and material
The data that support the findings of this study are available from the corresponding author upon reasonable request.

Author Contributions
Tahereh Naseriyeh (Conducting laboratory research and writing articles); Elham Arkan and Danial Kahrizi (Research design and Writing); Sajad Moradi (Data Analysis), Farzad Kahrizi (Technical support for research and editing).

Funding
This research has been funded by Razi University.

References

1. Gonzalez AC, Costa TF, Andrade ZA, Medrado AR (2016) Wound healing - A literature review. An Bras Dermatol 91(5): 614-620. doi: 10.1590/abd1806-4841.20164741.
2. Jeschke MG, Wood FM, Middelkoop E, Bayat A, Teot L, Ogawa R, Gauglitz GG (2023) Scars. Nat Rev Dis Primers 9(1): 64. doi: 10.1038/s41572-023-00474-x.
3. Greaves NS, Ashcroft KJ, Baguneid M, Bayat A (2013) Current understanding of molecular and cellular mechanisms in fibroplasia and angiogenesis during acute wound healing. J Dermatol Sci 72(3): 206-217. doi:10.1016/j.jdermsci.2013.07.008.
4. Rees PA, Greaves NS, Baguneid M, Bayat A (2015) Chemokines in wound healing and as potential therapeutic targets for reducing cutaneous scarring. Adv Wound Care 4(11): 687-703. doi: 10.1089/wound.2014.0568.
5. Profyris C, Tziotzios C, Do Vale I (2012) Cutaneous scarring: Pathophysiology, molecular mechanisms, and scar reduction therapeutics: Part I. The molecular basis of scar formation. J Am Acad Dermatol 66(1): 1-10. doi: 10.1016/j.jaad.2011.05.055.
6. Pakshir P, Noskovicova N, Lodyga M, Son DO, Schuster R, Goodwin A, Karvonen H, Hinz B (2020) The myofibroblast at a glance. J Cell Sci 133(13): jcs227900. doi:10.1242/jcs.227900.
7. Terunuma A, Aiba S, Tagami H (2001) Cytokine mRNA profiles in cultured human skin component cells exposed to various chemicals: a simulation model of epicutaneous stimuli induced by skin barrier perturbation in comparison with that due to exposure to haptens or irritant. J Dermatol Sci 26(2): 85-93. doi:10.1016/S0923-1811(00)00165-1.
8. Syed F, Ahmadi E, Iqbal SA, Singh S, McGrouther DA, Bayat A (2011) Fibroblasts from the growing margin of keloid scars produce higher levels of collagen I and III compared with intralesional and extralesional sites: clinical implications for lesional site-directed therapy. Br J Dermatol 164(1): 83-96. doi: 10.1111/j.1365-2133.2010.10048.x.
9. Sidgwick GP, Bayat A (2012) Extracellular matrix molecules implicated in hypertrophic and keloid scarring. J Eur Acad Dermatol Venereol 26(2): 141-152. doi: 10.1111/j.1468-3083.2011.04200.x.
10. Zhuang Z, Li Y, Wei X (2021) The safety and efficacy of intralesional triamcinolone acetonide for keloids and hypertrophic scars: A systematic review and meta-analysis. Burns 47(5): 987-998. doi: 10.1016/j.burns.2021.02.013.
11. Bijlard E, Steltenpool S, Niessen FB (2015) Intralesional 5-fluorouracil in keloid treatment: a systematic review. Acta Derm Venereol 95(7): 778-782. doi:10.2340/00015555-2106.
12. Muskat A, Kost Y, Balazic E, Cohen JL, Kobets K (2023) Laser-assisted drug delivery in the treatment of scars, rhytids, and melasma: a comprehensive review of the literature. Aesthet Surg J 43(3): NP181-NP198. doi:10.1093/asj/sjac286.
13. O'Boyle CP, Shayan-Arani H, Hamada MW (2017) Intralesional cryotherapy for hypertrophic scars and keloids: a review. Scars Burns Heal 3: 2059513117702162. doi: 10.1177/2059513117702162.
14. Ogawa R, Yoshitatsu S, Yoshida K, Miyashita T (2009) Is radiation therapy for keloids acceptable? The risk of radiation-induced carcinogenesis. Plast Reconstr Surg 124(4): 1196-1201. doi: 10.1097/PRS.0b013e3181b5a3ae.
15. Ogawa R, Dohi T, Tosa M, Aoki M, Akaishi S (2021) The latest strategy for keloid and hypertrophic scar prevention and treatment: the Nippon Medical School (NMS) protocol. J Nippon Med Sch 88(1): 2-9. doi:10.1272/jnms.JNMS.2021_88-106.
16. Berman B, Perez OA, Konda S, Kohut BE, Viera MH, Delgado S, Zell D, Li Q (2007) A review of the biologic effects, clinical efficacy, and safety of silicone elastomer sheeting for hypertrophic and keloid scar treatment and management. Dermatol Surg 33(11): 1291-1303. doi:10.1111/j.1524-4725.2007.33280.x.
17. Kim S, Choi TH, Liu W, Ogawa R, Suh JS, Mustoe TA (2013) Update on scar management: guidelines for treating Asian patients. Plast Reconstr Surg 132(6): 1580-1589. doi: 10.1097/PRS.0b013e3182a8070c.
18. Yim SJ, Nam DY, Choi DH, Woo J, Kim Y, Chae J, Lee YS, Jung JY (2024) Evaluation of silicone-based gel for the treatment of hypertrophic scarring in rat models. J Wound Manag Res 20(2): 122-127. doi: 10.22467/jwmr.2024.02901
19. Sawada Y, Sone K (1992) Hydration and occlusion treatment for hypertrophic scars and keloids. Br J Plast Surg 45(8): 599-603. doi:10.1016/0007-1226(92)90027-U.
20. Zeng G, Zhong F, Li J, Luo S, Zhang P (2013) Resveratrol-mediated reduction of collagen by inhibiting proliferation and producing apoptosis in human hypertrophic scar fibroblasts. Biosci Biotechnol Biochem 77(12): 2389-2396. doi:10.1271/bbb.130502.
21. Zhai XX, Ding JC, Tang ZM (2015) Resveratrol inhibits proliferation and induces apoptosis of pathological scar fibroblasts through the mechanism involving TGF-β1/Smads signaling pathway. Cell Biochem Biophys 71: 1267-1272. doi:10.1007/s12013-014-0336-4.
22. Tang ZM, Zhai XX, Ding JC (2017) Expression of mTOR/70S6K signaling pathway in pathological scar fibroblasts and the effects of resveratrol intervention. Mol Med Rep 15(5): 2546-2550. doi:10.3892/mmr.2017.6339.
23. Mehta M, Branford OA, Rolfe KJ (2016) The evidence for natural therapeutics as potential anti-scarring agents in burn-related scarring. Burns Trauma 4. doi: 10.1186/s41038-016-0040-1.
24. McClements DJ (2020) Advances in nanoparticle and microparticle delivery systems for increasing the dispersibility, stability, and bioactivity of phytochemicals. Biotechnol Adv 38: 107287. doi: 10.1016/j.biotechadv.2018.08.004.
25. Jain N, Gupta BP, Thakur N, Jain R, Banweer J, Jain DK, Jain S (2010) Phytosome: a novel drug delivery system for herbal medicine. Int J Pharm Sci Drug Res 2(4): 224-228. doi:10.22376/ijpsdr.2010.2.4.224-228.
26. Damle M, Mallya R (2016) Development and evaluation of a novel delivery system containing phytophospholipid complex for skin aging. AAPS PharmSciTech 17(3): 607-617. doi:10.1208/s12249-015-0390-2.
27. Gillet A, Compère P, Lecomte F, Hubert P, Ducat E, Evrard B, Piel G (2011) Liposome surface charge influence on skin penetration behavior. Int J Pharm 411(1-2): 223-231. doi: 10.1016/j.ijpharm.2011.03.049.
28. Sinico C, Manconi M, Peppi M, Lai F, Valenti D, Fadda A.M (2005) Liposomes as carriers for dermal delivery of tretinoin: in vitro evaluation of drug permeation and vesicle–skin interaction. J Control Release 103(1): 123-136. doi: 10.1016/j.jconrel.2004.11.020.
29. Kohli AK, Alpar HO (2004) Potential use of nanoparticles for transcutaneous vaccine delivery: effect of particle size and charge. Int J Pharm 275(1-2): 13-17. doi: 10.1016/j.ijpharm.2003.10.038.
30. Vu HT, Hook SM, Siqueira SD, Müllertz A, Rades T, McDowell A (2018) Are phytosomes a superior nanodelivery system for the antioxidant rutin? Int J Pharm 548(1): 82-91. doi:10.1016/j.ijpharm.2018.06.042.
31. Puri N, Talwar A (2009) The efficacy of silicone gel for the treatment of hypertrophic scars and keloids. J Cutan Aesthet Surg 2(2): 104-106. doi: 10.4103/0974-2077.58527.
32. Dyson E, Sikkink S, Nocita D, Twigg P, Westgate G, Swift T (2023) Evaluating the irritant factors of silicone and hydrocolloid skin contact adhesives using trans-epidermal water loss, protein stripping, erythema, and ease of removal. ACS Appl Bio Mater

7(1): 284-296. doi: 10.1021/acsabm.3c00874.
33. Lin MH, Hung CF, Sung HC, Yang SC, Yu HP, Fang JY (2021) The bioactivities of resveratrol and its naturally occurring derivatives on skin. J Food Drug Anal 29(1): 15. doi: 10.38212/2224-6614.1151.
34. Ha AT, Rahmawati L, You L, Hossain MA, Kim JH, Cho JY (2021) Anti-inflammatory, antioxidant, moisturizing, and antimelanogenesis effects of quercetin 3-O-β-D-glucuronide in human keratinocytes and melanoma cells via activation of NF-κB and AP-1 pathways. Int J Mol Sci 23(1): 433. doi: 10.3390/ijms23010433.
35. Chen Y, Wu Q, Zhang Z, Yuan L, Liu X, Zhou L (2012) Preparation of curcumin-loaded liposomes and evaluation of their skin permeation and pharmacodynamics. Molecules 17(5): 5972-5987. doi: 10.3390/molecules17055972.
36. Zvonar Pobirk A, Roškar R, Bešter-Rogač M, Gašperlin M, Gosenca Matjaž M (2024) The impact of phospholipid-based liquid crystals' microstructure on stability and release profile of ascorbyl palmitate and skin performance. Molecules 29(13): 3173. doi: 10.3390/molecules29133173.
37. Naseriyeh T, Kahrizi D, Alvandi H, Aghaz F, Nowroozi G, Shamsi A, Hosseini O, Arkan E (2023) Glycyrrhizic acid delivery system chitosan-coated liposome as an adhesive anti-inflammation. Cell Mol Biol 69(4): 1-6. doi: 10.14715/cmb/2023.69.4.1.
38. Naseriyeh T, Kahrizi D, Alvandi H, Rajati H, Behbood L, Khodabandeh Shahraky M, Arkan E (2022) Preparation of liposomal hydrogel containing Calendula and application as a wound dressing. Cell Mol Biol 68(11): 1-7. doi: 10.14715/cmb/2022.68.11.1.
39. Abdi F, Arkan E, Eidizadeh M, Valipour E, Naseriyeh T, Gamizgy YH, Mansouri K (2023) The possibility of angiogenesis inhibition in cutaneous melanoma by bevacizumab-loaded lipid-chitosan nanoparticles. Drug Deliv Transl Res 13(2): 568-579.
40. Bi Y, Xia H, Li L, Lee RJ, Xie J, Liu Z, Qiu Z, Teng L (2019) Liposomal vitamin D3 as an anti-aging agent for the skin. Pharmaceutics 11(7): 311. doi: 10.3390/pharmaceutics11070311.
41. Maione-Silva L, de Castro EG, Nascimento TL, Cintra ER, Moreira LC, Cintra BAS, Valadares MC, Lima EM (2019) Ascorbic acid encapsulated into negatively charged liposomes exhibits increased skin permeation, retention and enhances collagen synthesis by fibroblasts. Sci Rep 9(1): 522.
42. Mazumder A, Dwivedi A, Fox LT, Brümmer A, Du Preez JL, Gerber M, Du Plessis J (2016) In vitro skin permeation of sinigrin from its phytosome complex. J Pharm Pharmacol 68(12): 1577-1583. doi:10.1111/jphp.12594.
43. Kalita B, Das MK (2015) Resveratrol-phospholipid complexes (phytosomes) with improved physicochemical properties favorable for drug delivery via skin. World J Pharm Res 4(5): 1497-1517. doi: 10.20959/wjpr20155-4859.